Chapter 2

Synthetic Cationic Cholesteric Liquid Crystal Polymers

Mercedes Pérez Méndez

Additional information is available at the end of the chapter

http://dx.doi.org/10.5772/intechopen.70995

Abstract

We report the synthesis of six multifunctional cationic cholesteric liquid crystals polyesters functionalized with choline, amine, and amide groups to obtain new chemical formulations involving macromolecular features with new properties added to those of precursor chiral cholesteric polyesters. They are designed as PTOBDME-choline $[(C_{34}H_{36}O_8)_n{-}C_5H_{13}N]$; PTOBEE-choline $[(C_{26}H_{20}O_8)_n{-}C_5H_{13}N]$; PTOBDME-ammonium $[(C_{34}H_{36}O_8)_n{-}C_5H_{13}N]$; PTOBEE-ammonium $[(C_{26}H_{20}O_8)_n{-}C_5H_{13}N]$; PTOBUME-amide $(C_{33}H_{33}O_9N)_n$; and PTOBEE-amide $(C_{26}H_{19}O_9N)_n$. Structural characterization is performed by NMR. Thermal behavior is studied by thermogravimetry (TG) and differential scanning calorimetry (DSC), showing all the polymers endothermic transition from crystal phase to liquid crystal mesophase. Chirality is determined by optical rotatory dispersion (ORD). The cationic cholesteric liquid crystal polymers described here have proved to act as nonviral vectors in gene therapy, transfecting DNA to the nucleus cell.

Keywords: cholesteric LC, cationic polymers, chiral polyesters, synthesis, NMR, DSC

1. Introduction

Cholesteric liquid crystal polyesters have received much attention in the last few years for their interesting chemical, optical, mechanical, and biological properties. Due to their anisotropic formulation and amphiphilic nature, their molecules are able to self-associate and/or aggregate in blocks to form species with supramolecular ordered structure, which presents desirable material properties.

Two cholesteric liquid crystal polyesters, named PTOBDME and PTOBEE in **Figure 1**, were obtained by polycondensation reaction. Although only racemic materials were used in their synthesis, a cholesteric, chiral morphology, theoretically unexpected, was found. Evidence of this was obtained when a white solid, recrystallized, as the second fraction, from toluene mother

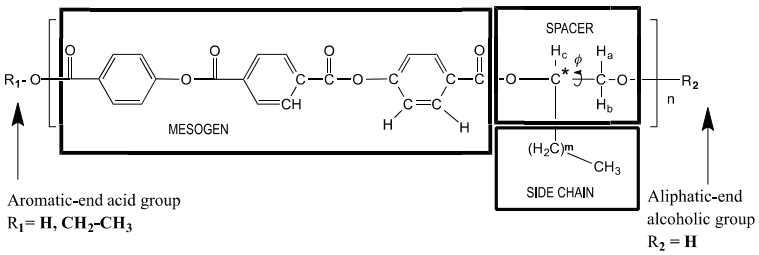

Figure 1. Monomeric unit of cholesteric liquid-crystalline PTOBEE (m = 1) and PTOBDME (m = 9). The three different zones of the monomer: *mesogen*, *spacer*, and *flexible side chain* are indicated. The asterisk indicates the chiral center. Torsion angle φ, along the bond containing the asymmetric carbon atom, is indicated. Aromatic-end acid and aliphatic-end alcoholic groups are also specified.

liquor after the filtration of the polymer, was identified as –PTOBDME, with $[\alpha]^{25}_{589} = -1.43$ (1.538g/100 ml, toluene) [1, 2] and –PTOBEE, with a value of $[\alpha]^{25}_{589} = -2.33$ (0.0056 mol/l, toluene) [3], respectively. The synthetic method [4], based on the previously reported by Bilibin [5], leads to obtain two or more fractions of different kinetic rates, with different enantiomeric excess. Not always, the enantiomer in excess is the same.

We are interested in the molecular design and chemical modifications of these multifunctional cholesteric liquid crystals to obtain new chemical formulations involving macromolecular features with new properties added. Our main interest being to introduce cationic charge, hence favoring the creation of hydrogen bonds, through intra and intermolecular interactions, giving secondary structures with long-range supramolecular order, and enabling to interact with molecules of interest, such as biological molecules (lipids, DNA, and oligonucleotides) and metal surfaces. The functional groups selected to be introduced at the end of the main chains were Choline [–CH_2–CH_2–N–$(CH_3)_3$] and ammonium [–CH_2–CH_2–CH_2–NH–$(CH_3)_2$] and amide groups (–$CONH_2$) at the end of the lateral hydrophobic chains.

The new synthetized cationic polymers reported here have proved to be able to interact with negatively charged DNA, forming polyplexes, which are able to condense and successfully transfect the new DNA into the nucleus cell, protecting it from damage during the transfection process, acting as nonviral vectors in Gene Therapy [6, 7]. Besides, they are sensitive to pH changes, acting as polycationic efficient transfection agents possessing substantial buffering capacity below physiological pH. These vectors have shown to deliver genes as well as oligonucleotides, both *in vitro* and *in vivo*, by protecting DNA from inactivation by blood components. Their efficiency relies on extensive endosome swelling and rupture that provides an escape mechanism for the polycation/DNA complexes [8].

2. Materials

The new cholesteric liquid crystal polymers so designed have been synthesized as follows: PTOBDME-choline $[(C_{34}H_{36}O_8)_n–C_5H_{13}N]$; PTOBEE-choline $[(C_{26}H_{20}O_8)_n–C_5H_{13}N]$; PTOBDME-ammonium $[(C_{34}H_{36}O_8)_n–C_5H_{13}N]$; PTOBEE-ammonium $[(C_{26}H_{20}O_8)_n–C_5H_{13}N]$; PTOBUME-amide $[(C_{33}H_{33}O_9N)_n$; and PTOBEE-amide $(C_{26}H_{19}O_9N)_n$.

2.1. Synthesis of cholesteric PTOBDME-choline [$(C_{34}H_{36}O_8)_n$–$C_5H_{13}N$]

Poly[oxy(1,2-dodecane)oxycarbonyl-1,4-phenylene-oxy-1,4-terephthaloyl-oxy-1,4-phenylene-carbonyl]-oxy-*N*, *N*, *N*-trimethylethan-1-ammonium (Choline) chloride, **II** in **Figure 2**, was obtained through polycondensation reaction between: 4,4′-(terephthaloyldioxydibenzoic

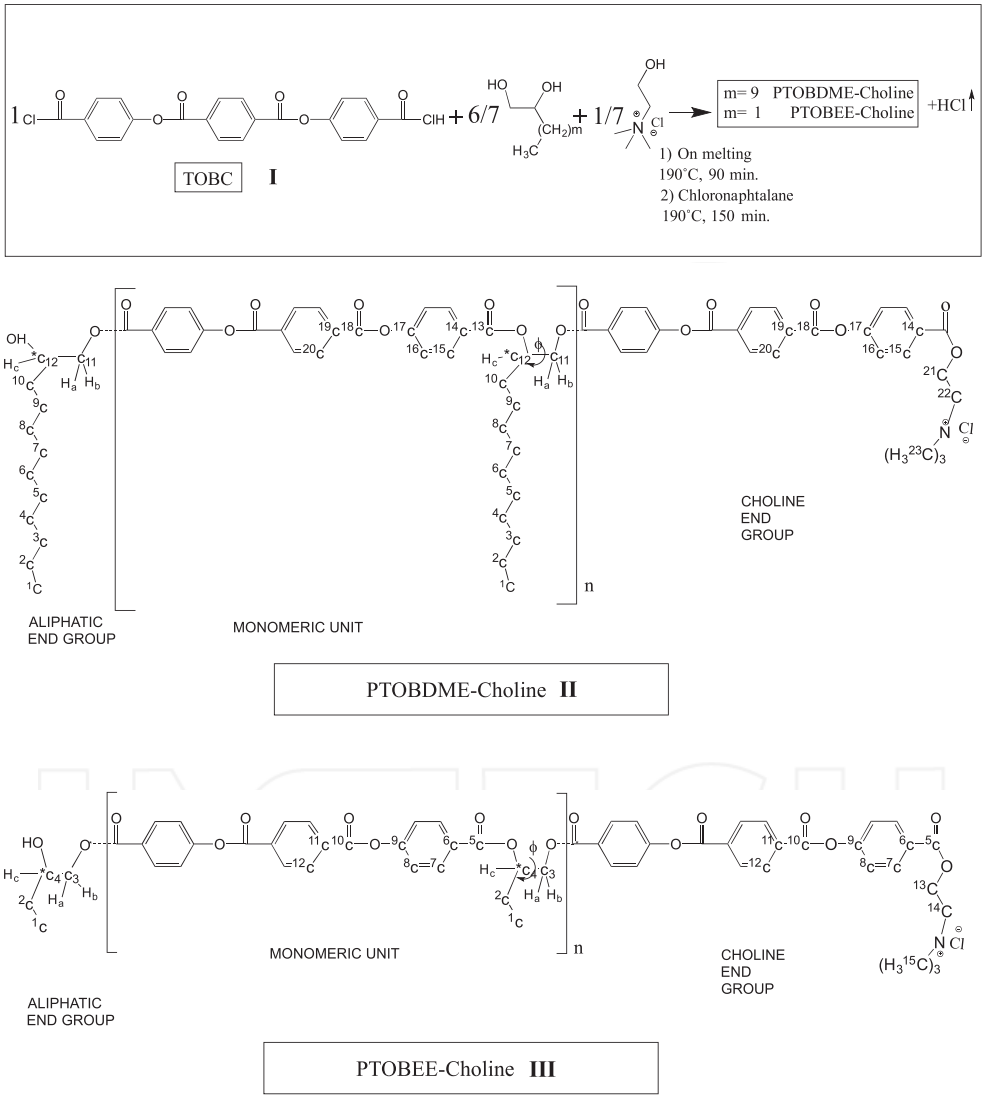

Figure 2. Synthetic process of cholesteric liquid-crystalline PTOBDME-choline (m = 9) (II) and PTOBEE-choline (m = 1) (III). Monomeric units are indicated, together with aliphatic end groups and choline aromatic end groups. The asterisks indicate the chiral centers ($^{12}C^*$) and ($^{4}C^*$), respectively. Torsion angles φ, along (^{12}C—^{11}C) and (^{4}C—^{3}C) bonds, respectively, are shown.

chloride) **TOBC**, **I** in **Figure 2**, the racemic mixture of DL-1,2-dodecanediol, and choline chloride. Notation similar to precursor cholesteric liquid crystal PTOBDME [1, 2] is used.

2.2. Synthesis of cholesteric PTOBEE-choline [$(C_{26}H_{20}O_8)_n$—$C_5H_{13}N$]

The structure of Poly[oxy(1,2-butane)oxycarbonyl-1,4-phenylene-oxy-1,4-terephthaloyl-oxy-1,4-phenylene-carbonyl]-oxy-*N*,*N*,*N*-trimethylethan-1-aminium (choline) chloride is shown in **III** of **Figure 2**. The polycondensation included DL-1,2-butanediol. Notation similar to precursor cholesteric liquid crystal PTOBEE [3, 4] is used.

2.2.1. Preparation of PTOBDME-choline and PTOBEE-choline

The dichloride, TOBC, was obtained by reaction between thionyl chloride and 4,4′-(terephthaloyldioxydibenzoic) acid (TOBA), previously synthesized from terephthaloyl chloride and 4-hydroxybenzoic acid [5].

The polycondensation reaction between TOBC and the racemic mixture, the corresponding glycol, takes place in presence of 1/7 equimolecular choline chloride. The preparation of these compounds was performed on melting due to the insolubility of choline chloride in the solvents used in the synthesis of PTOBDME or PTOBEE precursors, diphenyl oxide, or chloronaphthalene.

A mixture of 0.0054 mol of the glycol, either DL-1,2-dodecanediol or DL-1,2-butanediol, from Flucka Chemie GmBH (Buchs, Switzerland) and 0.000775 mol of choline chloride from Sigma-Aldrich Chemie GmBH (Steinheim, Germany) were placed into a flask of 50 ml contained in a bath with a high-temperature transfer agent, while a current of dry nitrogen from Praxair (Madrid, Spain) was used to purge the system at room temperature and then maintained in the rest of the reaction. The mixture was stirred and heated to 110°C to whole dissolution of the choline chloride into diol. The bath was cooled to 80°C, and 0.0062 mol of TOBC was added; this temperature was maintained for 15 minutes. The bath was heated up to 190°C, the mixture was melted, and emission of HCl was observed. After 60 minutes, 15 ml of chloronaphthalene from Sigma-Aldrich Chemie GmBH (Steinheim, Germany) was added. The reaction mix was maintained into the solvent stirring at 190°C for 150 minutes. Then, it was poured into 150 ml of toluene from Merck KGaA (Darmstadt, Germany), decanting PTOBDME-choline or PTOBEE-choline, respectively, which was filtered, washed with ethanol, and vacuum dried.

2.3. Synthesis of cholesteric PTOBDME-ammonium [$(C_{34}H_{36}O_8)_n$—$C_5H_{13}N$]

The structure of Poly[oxy (1,2-dodecane)-oxy-carbonyl-1,4-phenylene-oxy-1,4-terephthaloyl-oxy-1,4-phenylene-carbonyl]-oxy-3-dimethyl amine-1-propyl choride is shown in **II** of **Figure 3**.

2.4. Synthesis of Cholesteric PTOBEE-ammonium [$(C_{26}H_{20}O_8)_n$—$C_5H_{13}N$]

The structure of Poly[oxy(1,2-butane)oxycarbonyl-1,4-phenylene-oxy-1,4-terephthaloyl -oxy-1,4-phenylene-carbonyl]-oxy-3-dimethylamine-1-propyl choride is shown in **III** of **Figure 3**.

2.4.1. Preparation of PTOBMDE-ammonium and PTOBEE-ammonium

PTOBDME-ammonium chloride, **II** in **Figure 3**, and PTOBEE-ammonium chloride, **III** in **Figure 3**, were obtained through polycondensation reaction between 4 and 4′-(terephthaloyl-dioxydibenzoic chloride) **TOBC**, **I** in **Figure 3**, and the racemic mixture of **DL-1,2-dodecanediol** and **DL-1,2-butanediol,** respectively, and then reaction with 3-Dimethylamino-1-propanol. Notation of cholesteric liquid crystal PTOBDME and PTOBEE precursors is used. Next, a typical preparation of PTOBDME-ammonium chloride is shown.

Into a flask of 50 ml, TOBC (0.0079 mol) and 1,2-dodecanediol (0.0079 mol) from Flucka Chemie GmBH (Buchs, Switzerland) and diphenyl oxide (19.7 ml) of from Sigma-Aldrich Chemie GmBH (Steinheim, Germany) were mixed, while the system was purged with stream of dry nitrogen from Praxair (Madrid, Spain), for 30 min at room temperature. Then, while maintaining the gas current, the flask was transferred to a bath at 200°C for 2 hours; since the liberation of HCl is still observed, the temperature of the bath was descended to 160°C, the polycondensation was stopped and was not observed HCl formation. 3-Dimethylamino-1-propanol (0.2 ml, 0.00156 mol) was added to the reaction mix, and the liberation of HCl returned again. After 2 hours, the reaction finished. The result of the polycondensation reaction was poured into 200 ml of toluene from Merck KGaA (Darmstadt, Germany), decanting PTOBDME, which was filtered, washed with ethanol, and vacuum dried.

2.5. Synthesis of cholesteric PTOBUME-amide $[(C_{33}H_{33}O_9N)_n$

Poly[oxy(1,2-undecan-11-amidyl)-oxycarbonyl-1,4-phenylene-oxy-1,4-terephthaloyl-oxy-1,4-phenylene-carbonyl], **VII** in **Figure 4**, was obtained through polycondensation reaction between 4 and 4′-(terephthaloyldioxydibenzoic chloride) **TOBC** and the racemic mixture of **DL-10,11-dihydroxyundecanemide** (**V** in **Figure 4**) [11–15]. Similar notation has been used than with precursor cholesteric liquid crystal PTOBDME, **Figure 1**.

*2.5.1. Preparation of undec-10-enoyl chloride (**II** in **Figure 4**)*

To a stirred solution of 0.118 mol of undec-10-enoic acid in 100 ml of toluene, at 25°C, 0.078 mol of oxalyl chloride was added during 30 minutes. The solution was stirred for 30 minutes after emission of HCl gas had completed. The mixture reaction was concentrated to about half the initial volume by using a vacuum pump equipped with a sodium hydroxide trap. This solution was used directly to prepare undec-10-enamide (**III** in **Figure 4**).

2.5.2. Preparation of undec-10-enamide

A NH_3 gas stream was used to purge the stirred solution of undec-10-enoyl chloride, cooled in a bath of dry ice/acetone. The NH_3 stream was produced by boiling to reflux ammonia solution generated by reaction between 100 g of $ClHN_4$ solved into 300 ml of H_2O and 76 g of NaOH solved in 50 ml of water at 10°C. The reflux condenser and a NaOH trap were connected between the ammonia solution and the mixture reaction to prevent moisture. After 30 minutes of reaction, when a white solid had precipitated and HCl gas emission was not

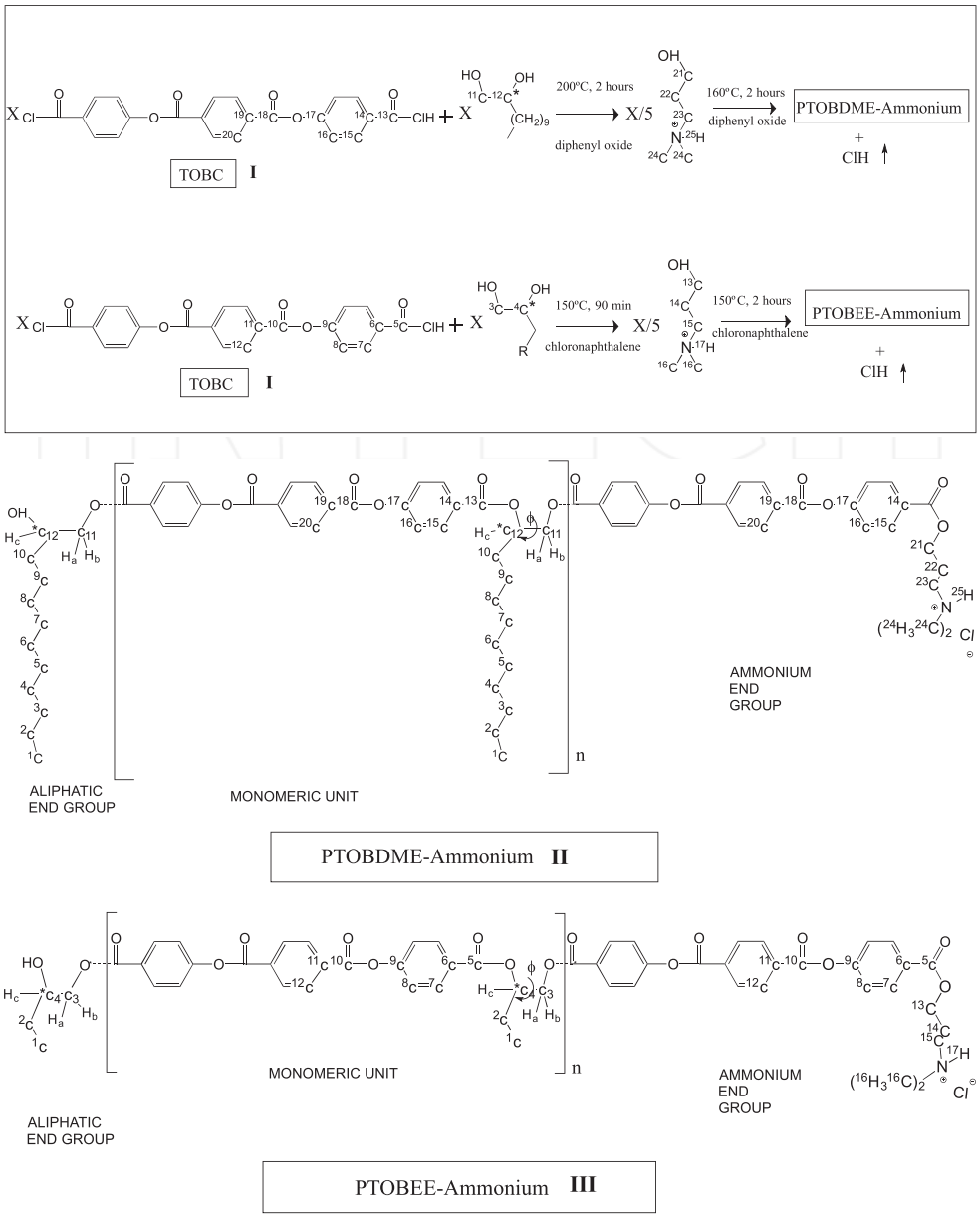

Figure 3. Synthetic process of cholesteric liquid-crystalline PTOBDME-ammonium (II), and PTOBEE-ammonium (III). Monomeric units are indicated, together with aliphatic end groups and ammonium aromatic end groups. The asterisks indicate the chiral centers ($^{4}C^{*}$) and ($^{12}C^{*}$), respectively. Torsion angles φ, along ($^{4}C—^{3}C$) and ($^{12}C—^{11}C$) bonds, are shown.

observed, the reaction flask was allowed to warm to room temperature. The mixture reaction was concentrated to a residue on a rotatory evaporator. The solid was partitioned between 10% aqueous sodium hydroxide and dichloromethane, and the aqueous phase was washed

three times with additional dichloromethane. The combined dichloromethane extracts were washed with brine, dried with anhydrous sodium sulfate, and concentrated to a solid on a rotatory evaporator [12–15]. The solid was recrystallized in a mix chloroform/hexane (1:1) to give pure undec-10-enamide—yield (80%) and melting point 87°C (**III** in **Figure 4**).

^{1}H NMR ($CDCl_3$ 300 MHz, δ; (ppm)): δ 7.19, (dd, 2H) *(7.03)*, δ 5.80, (m, 1H) *(5.82)*, δ 5.32-5.22, (bs, 1H,) *(5.13)*, δ 4.96, (dd, 1H J = 7.2 Hz) *(4.88)*, δ 2.21, (t, 2H, J = 7.6 Hz) *(2.34)*; δ 2.02 *(2.13)*, (m, 2H), δ 1.62 (t, 2H, J = 7.4 Hz) *(1.53)*, δ 1.33-1.28, overlapped (10H) *(1.33, 1.30, 1.30, 1.30, 1.29)*. In tilted numbers are the calculated shifts.

^{13}C NMR ($CDCl_3$ 100 MHz, δ; (ppm)): 175.2 *(173.6)*, 139.6 *(139.1)*, 114.5 *(115.7)*, 36.3 *(38.7)*, 34.2 *(33.9)*, 29.4 *(29.7, 29.7, 29.6, 28.9, 28.6)* and 25.4 *(25.3)*. HRMS m/z calc. For $C_{11}H_{21}NONa$ + [M + Na] + 206.2; found 206.2.

2.5.3. Preparation of 10-11 epoxy undecanamide

To a stirred solution of undec-10-enamide (7 g;) in 108.4 ml of acetone, $NaHCO_3$ (26.4 g) was added, and then, 5.2 ml of water was added carefully. The resultant thick mixture was strongly stirred, while a solution of 40.6 g of oxone in 158 ml of water was added dropwise during 45 min. The reaction was monitored by thin layer chromatography (TLC) using a mix of ethyl acetate/hexane 2:1. After the reaction was complete, the acetone was removed by evaporation. The remaining solution was acidified with HCl 10% to pH 2 at 10°C and followed rapid extraction with 250 ml of dichloromethane. The aqueous phase was washed three times with additional dichloromethane. The combined organic phase was washed with brine, dried with anhydrous sodium sulfate, and concentrated to a white solid on a rotatory evaporator (**IV** in **Figure 4**).

^{1}H NMR ($CDCl_3$ 300 MHz, δ; (ppm)): δ 5.44, (bs, 2H), δ 2.90, (m, 1H), δ 2.74, (dd, 1H J = 4.6 Hz), δ 2.46, (dd, 1H J = 5.0 Hz), δ 2.21, (t, 2H, J = 7.6 Hz); δ 1.62 (t, 2H, J = 7.4 Hz), δ 1.51, (m, 2H), δ 1.44 (m, 2H), δ 1.33-1.28, (bs, 8H); ^{13}C NMR ($CDCl_3$ 100 MHz, δ; (ppm)): 173.8 (1C) (**C**$CONH_2$), 137.6 (1C) (═**C**H─C), 115.7 (1C) (H_2**C**═), 38.7 (1C) (─H_2**C**─$CONH_2$), 29.7 (3C), 28.7 (2C), 25.3 (1C); HRMS m/z calc. For $C_{11}H_{21}NO_2Na$ + [M + Na]+; found.

2.5.4. Preparation of 10-11 of dihydroxyundecanamide

The previously obtained 10-11 epoxy undecanamide was stirred during 8 hours at 60°C in aqueous HCl 10%. The reaction was monitored by TLC using a mix of ethyl acetate/hexane 2:1. An oil, not miscible with water, was obtained. The mixture reaction was extracted with dichloromethane, and the aqueous phase was washed three times with additionally dichloromethane. The combined organic phase was washed with brine, dried with anhydrous sodium sulfate, and concentrated to a yellow oil on a rotatory evaporator. Yield (75%) (**V** in **Figure 4**).

^{1}H NMR ($CDCl_3$ 300 MHz, δ; (ppm)): δ 5.44, (bs, 2H), δ 3.78, (m, 1H), δ 3.60, (dd, 1H J = 11.0 Hz), δ 3.48, (dd, 1H J = 2.21, (t, 2H, J = 7.6 Hz); δ 1.62 (t, 2H, J = 7.4 Hz);), δ 1.51, (m, 2H), δ 1.44 (m, 2H), δ 1.33-1.28, (bs, 8H);

^{13}C NMR ($CDCl_3$ 100 MHz, δ; (ppm)): HRMS m/z calc. For $C_{11}H_{23}NO_3H_3O$+ [M + H_3O] + 236.2; found 236.2.

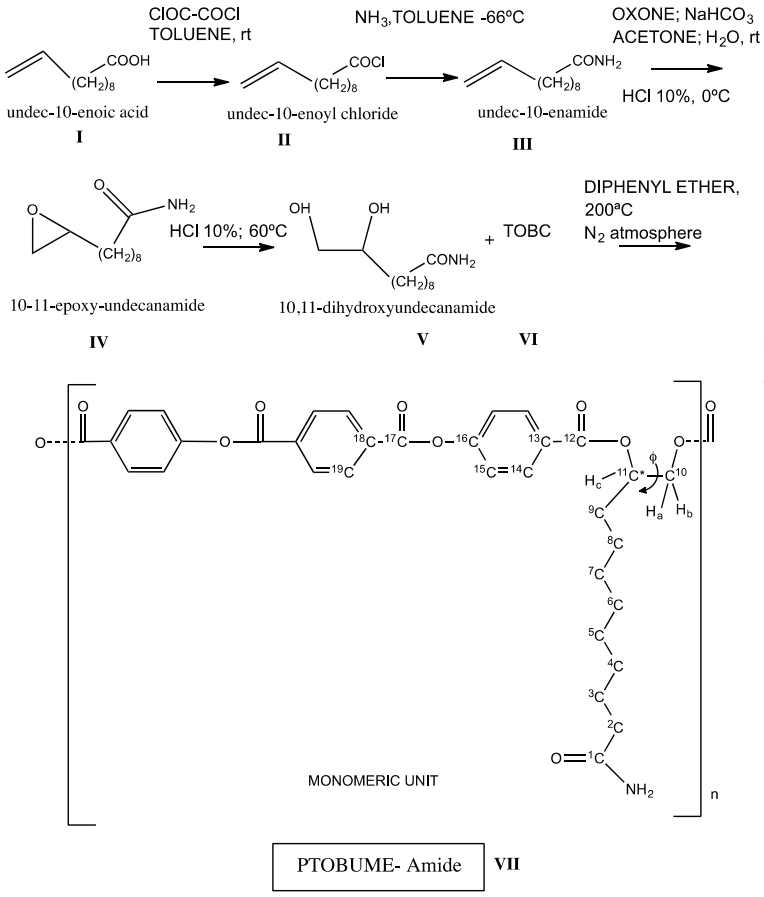

Figure 4. Synthetic method of cholesteric liquid-crystalline PTOBUME-amide. The asterisk indicates the chiral center ($^{11}C^*$). Torsion angle φ, along $^{10}C—^{11}C$ bond.

2.5.5. Preparation of TOBC

In the course of 20 minutes, 20 g TOBA were added to 350 ml thionyl chloride from Sigma-Aldrich Chemie GmBH (Steinheim, Germany), while stirring rapidly at room temperature (**VI** in **Figure 4**).

The solution was boiled with the reflux condenser. When the emission of HCl had finished and most of the sediment had dissolved, the hot solution was filtered and cooled down to 0°C for a day. The obtained product that separated out was filtered, vacuum dried, and recrystallized in chloroform, from SDS Votre Partenaire Chimie (Peypin, France).

Yield: 14 g (60%).

2.5.6. Preparation of PTOBUME-amide.

A mixture of TOBC (5.5 g; 0.012 mol), 10-11 of dihydroxyundecanamide (2.7 g; 0.012 mol) in 3 ml of diphenyl oxide from Sigma-Aldrich Chemie GmBH (Steinheim, Germany) was purged with dry nitrogen from Praxair (Madrid, Spain) for 25min at room temperature. Then, while maintaining the gas stream, the flask was transferred to a bath containing a high-temperature heat-transfer agent. The polycondensation was carried out for 360 minutes at 200°C. The reaction gets completed when emission of HCl had finished. The reaction mixture was poured into 300 ml of toluene from Merck KGaA (Darmstadt, Germany), decanting PTOBUME-amide. After 12 hours, it was filtered, washed with ethanol, and vacuum dried. After 3 weeks, a second fraction of polymer was precipitated of the toluene mother liquors, which was filtered, washed with ethanol, and vacuum dried.

Yield first fraction 3.0 g (38.5%); yield first and second fraction 0.1 g (40.0%).

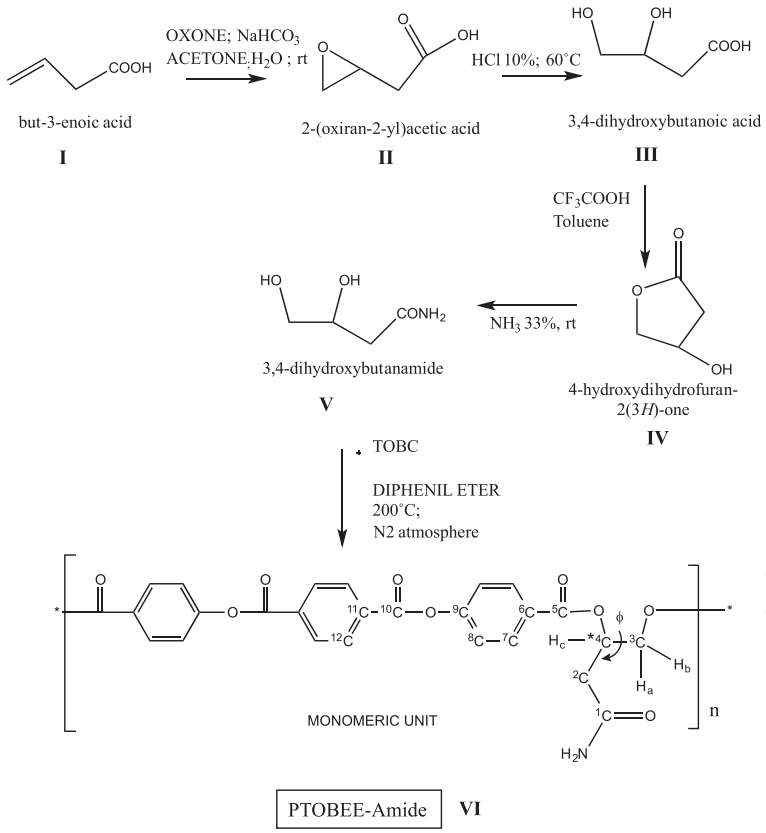

Figure 5. Synthetic method of cholesteric liquid-crystalline PTOBEE-amide.

2.6. Synthesis of Cholesteric PTOBEE-amide $(C_{26}H_{19}O_9N)_n$

Poly[oxy(1,2-butan-4-amidyl)-oxycarbonyl-1,4-phenylene-oxy-1,4-terephthaloyl-oxy-1,4-phenylene-carbonyl], **VI** in **Figure 5**, was obtained through poly-condensation reaction between 4 and 4′-(terephthaloyldioxydibenzoic chloride) **TOBC** and the racemic mixture of **DL-3,4-dihydroxybutanamide** (**IV** in **Figure 5**). The same notation has been used with precursor cholesteric liquid crystal PTOBEE, **Figure 1**.

2.6.1. Preparation of 3,4-dihydroxybutanoic acid

To a stirred mixture of 10 g of but-3-enoic acid solved in 130 ml acetone, 34 g. $NaHCO_3$ in 65 ml mili-Q water was added carefully. The resultant mixture was strongly stirred, while a solution of 51.1 g oxone in 200 ml of water was added dropwise during 120 min. The reaction was monitored by thin layer chromatography (TLC) using a mix of ethyl acetate/diethyl ether 1:1. After the reaction was complete, the acetone was removed by evaporation. The remaining solution was acidified with HCl 10% to pH 2 at 10°C and followed of rapid extraction with 250 ml of ethyl acetate. The aqueous phase was washed three times with additional ethyl acetate. The combined organic phase was washed with brine, dried with anhydrous sodium sulfate, and concentrated to a white solid on a rotatory evaporator (**III** in **Figure 5**).

2.6.2. Preparation of 4-hydroxydihydrofuran-2(3H)-one

To 3,4-dihydroxybutanoic acid into a flask equipped with a Dean Stark adapter filled with a toluene column finally connected to a refrigerant, 0.5 ml trifluoroacetic acid was added in 100 ml toluene heating to 110°C, mixing for 3 hours. The reaction product was removed with ethanol, washed in ethyl acetate, and dried. The reaction was monitored by thin layer chromatography (TLC) using a mix of ethyl acetate/diethyl ether 1:1 (**IV** in **Figure 5**).

2.6.3. Preparation of 3,4-dihydroxybutanamide

To the 4-hydroxydihydrofuran-2(3*H*)-one, 100 ml NH_3 33% was added stirring at 70°C with reflux for 12 h. The reaction product was removed with ethanol, filtered, and washed with water several times (**V** in **Figure 5**).

2.6.4. Preparation of PTOBEE-amide

In a three-neck round-bottom flask, 0.2 g 3,4-dihydroxybutanamide was added dropwise to 1 g TOBC solved in 100 ml 1,1,2,2-Tetrachloroethane. The reaction was stirred at 90°C for 20 hours. The reaction product was filtered, washed in 50 ml ethanol, 100 ml water, 200 ml $NaHCO_3$ (10%), 200 ml HCl (5%), 300 ml water, and 200 ml ethanol, and dried.

3. Characterization techniques

3.1. Conventional NMR techniques

The obtained polymers are characterized by ^{1}H-NMR, ^{13}C-NMR, COSY (Homonuclear Correlation Spectroscopy), TOCSY (Total Correlation Spectroscopy), NOESY (Nuclear Overhauser Effect

Spectroscopy, through-space correlation method), HSQC (Heteronuclear Single-Quantum Correlation spectroscopy), and HMBC (Heteronuclear Multiple Bond Correlation) for correlations between carbons and protons that are separated by two, three, and sometimes four bonds, in conjugated systems. Direct one-bond correlations being suppressed.

The experiments were performed in a Bruker 300 MHz NMR spectrometer and VARIAN 400 and 500 MHz spectrometers. The solvents used were DMSO-d_6 and $CDCl_3$, from Merck KGaA (Darmstadt, Germany), at 25°C. ^{1}H chemical shifts were referenced to the residual solvent signal at δ = 2.50 ppm (DMSO-d_6) relative to tetramethylsilane (TMS). All the spectra were processed and analyzed with MestReNova v.11.0.4 software [9]. Predicted ^{1}H and ^{13}C-NMR chemical shifts were calculated from the formula with ChemDraw Professional, v.15.1.0.144 [10].

3.2. Thermal behavior

Thermal stability was studied by Thermogravimetry on a Mettler TA4000-TG50 at heating rate of 10°C/min with nitrogen purge between 30 and 600°C. Thermal behavior was determined by differential scanning calorimetry (DSC) in a Mettler TA4000/DSC30/TC11 calorimeter, with series of heating/cooling cycles in a temperature range between 0 and 230°C.

3.3. The optical activity

The optical activity of the polymers was measured as optical rotatory dispersion (ORD) at 25°C in DMSO from Scharlau Chemie, in a Perkin Elmer 241 MC polarimeter with wavelengths: λ_{Na} = 589 nm, slit = 5 mm, integration time = 50 s; λ_{Hg} = 574 nm, slit = 14 mm, integration time = 50s; λ_{Hg} = 546 nm, slit = 30 mm, integration time = 50 s; λ_{Hg} = 435 nm, slit = 5 mm, integration time = 50s; λ_{Hg} = 365 nm, slit = 2.5 mm, integration time = 50 s.

4. Structural characterization by NMR

4.1. Structural characterization of PTOBDME-choline

The designation of the ^{1}H and ^{13}C-NMR chemical shifts, in DMSO-d_6, of the monomeric unit and the end groups of Polyester PTOBDME-choline, is given in **Table 1**. All the spectra have been analyzed and interpreted the help of MestReNova [9]. The predicted theoretical values, also in **Table 1**, have been calculated by ChemDraw [10]. Similar notations as those assigned with precursor cholesteric liquid crystal polyesters PTOBDME [1, 2] have been used.

Considering the monomer structure, three zones can be differentiated in the ^{1}H-NMR spectrum, corresponding to *the mesogen*, including aromatic protons between 11.0–7.00 ppm, *the spacer* where methylene and methine protons directly attached to oxygen atoms are observed, with signals between 6 and 3 ppm, and *the flexible side chain* formed by aliphatic protons between 2 and 0.8 ppm. The main feature of the proton spectrum is the presence of higher number of peaks than those expected for the monomeric unit. Hydrogen atoms H_a and H_b are bonded to 11C atom, allocated in α position with respect to the asymmetric carbon atom ^{12}C*. For that reason, they are diastereotopic and their 1H-NMR signals, usually indistinguishable, split in two easily differentiated. The same effect is observed for H_d and H_e, bonded to ^{10}C, and for H_f and H_g, both bonded to ^{9}C.

Set of signal of system (′) and (″)				Set of signal of system without apostrophe ( )				Calculated chemical shift	
Atom	**^{1}H(ppm)**	**Atom**	**^{13}C(ppm)**	**Atom**	**^{1}H(ppm)**	**Atom**	**^{13}C(ppm)**	**^{1}H(ppm)**	**^{13}C(ppm)**
$^{20\prime}$H	8.36	$^{20\prime}$C	130.4	^{20}H	8.36	^{20}C	130.4	8.04	130.2
		$^{19\prime}$C	133.3			^{19}C	133.3		135.4
		$^{18\prime}$C	163.5			^{18}C	163.4		165.2
		$^{17\prime}$C	153.9			^{17}C	154.4		155.6
$^{16\prime}$H	7.50	$^{16\prime}$C	122.1	^{16}H	7.55	^{16}C	122.2	7.26	121.5
$^{15\prime}$H	8.08	$^{15\prime}$C	130.8	^{15}H	8.15	^{15}C	131.0	8.13, 8.11	130.3
		$^{14\prime}$C	128.8			^{14}C	127.6		126.9
		$^{13\prime}$C	166.7			^{13}C	164.7		165.9
H_c'	5.45	$^{12\prime}$C	72.3	H_c	5.26	^{12}C	73.7	4.55	70.3
H_c''	4.39	$^{12\prime\prime}$C	60.0					3.81	70.8
$H_a'H_b'$	4.63, 4.52	$^{11\prime}$C	65.7	$H_{a'}$ H_b	3.95, 3.89	^{11}C	46.4	4.80, 4.55	67.5
$H_a''H_b''$	4.52	$^{11\prime\prime}$C	67.8					4.53, 4.28	70.8
H_d'	1.83	$^{10\prime}$C	30.0	H_d	1.77	^{10}C	31.2	1.71	30.7
H_d'',H_e''	1.92 1.78	$^{10\prime\prime}$C						1.44	34.0
H_f', H_g'	1.45	$^{9\prime}$C	24.6	$H_{f'}$ H_g	1.35	^{9}C	24.4	1.29	23.3
H_f'', H_g''	1.53, 1.44	$^{9\prime\prime}$C	25.6					1.29	23.1
$^{8\prime}$H	1.24	$^{8\prime}$C	28.9 m*	^{8}H	1.24	^{8}C	28.9 m*	1.29	29.6
$^{7\prime}$H	1.24	$^{7\prime}$C	28.9 m*	^{7}H	1.24	^{7}C	28.9 m*	1.29	29.6
$^{6\prime}$H	1.24	$^{6\prime}$C	28.9 m*	^{6}H	1.24	^{6}C	28.9 m*	1.26	29.6
$^{5\prime}$H	1.24	$^{5\prime}$C	28.9 m*	^{5}H	1.24	^{5}C	28.9 m*	1.26	29.6
$^{4\prime}$H	1.24	$^{4\prime}$C	28.6 m*	^{4}H	1.24	^{4}C	28.6 m*	1.26	29.3
$^{3\prime}$H	1.24	$^{3\prime}$C	31.3	^{3}H	1.24	^{3}C	31.3	1.26	31.8
$^{2\prime}$H	1.24	$^{2\prime}$C	22.1	^{2}H	1.24	^{2}C	22.1	1.26	22.7
$^{1\prime}$H	0.85	$^{1\prime}$C	14.0	^{1}H	0.85	^{1}C	14.0	0.86	14.1

The symbol (′) and without it ( ) distinguish the two independent system of the repeating unit, the symbol (″) is used to mark signals due to the aliphatic end group. *Signal of ^{4}C to ^{8}C at 28.8 ppm is a multiplet from 28.9 to 28.6.

Table 1. ^{1}H and ^{13}C-NMR chemical shifts (ppm) observed and calculated for the repeating unit and the aliphatic end group polyester PTOBDME-choline.

The presence of two independent ^{1}H-NMR sets of signals are observed in the spectrum, one marked with (′) and the other without it ( ). They are attributed to two conformers *gg* and *gt* of the spacer within the repeating unit respectively. The same effect has been reported for PTOBDME and PTOBEE, and accordingly, similar nomenclature is used to identify the signals. A third set of signals, marked with (″), is assigned to the aliphatic end group.

In the aromatic zone singlet at 8.36 ppm belongs to ^{20}H and doublets at 7.50 and 8.08 ppm are assigned to $^{16'}H$ and $^{15'}H$, respectively, and doublets at 7.55 and 8.15 ppm to ^{16}H and ^{15}H; similar assignation was previously carried out in precursor PTOBDME [1]. In the spacer zone, multiplet at 5.45 ppm is interpreted due to H_c', and the double doublets at 4.63 and 4.52 ppm correspond to H_a' and H_b'. These peaks presented correlation signals in COSY and were related with other aliphatic signals $H_d'H_e'$ (1.83 ppm) and $H_f'H_g'$ (1.45 ppm) by TOCSY experiment. Multiplet at 5.26 ppm was assigned to H_c and double doublets at 3.95 and 3.89 ppm to H_a and H_b, and they showed COSY correlations and were related with signals at 1.77 ppm (H_d) and 1.35 ppm (H_f H_g) respectively by TOCSY experiment. The peaks assigned to H_a'', H_b'', and H_c'' due to aliphatic end group are overlapped with H_b' (4.52 ppm) and with ^{21}H (4.54 ppm) (in **Table 2**), and they were assigned through TOCSY correlations observed for signal at 4.52 ppm (not observed for 4.63 ppm, H_a'), with the multiplet at 4.39 ppm (H_c'') and confirmed by HSQC. By this method, carbon $C^{11'}$ (65.7 ppm) was correlated with signals at 4.63 (H_a') and 4.52 (H_b') and carbon $^{11''}C$ (67.8 ppm) with 4.52 ppm (H_a'') and (H_b''). Signals at 1.83 and 1.45 ppm assigned to (H_d') and (H_f', H_g') and correlated by COSY with H_c'(5.45 ppm). Peaks at 1.77 ppm (H_d H_e) and 1.35 ppm (H_f H_g) are correlated by COSY with H_c (5.26 ppm). Signals at 1.92, 1.78 ppm are related with H_c'' (4.39 ppm) by COSY experiments, and they were assigned to H_d'' and H_e''. They are also related with Hf" (1.53 ppm) and Hg"(1.44 ppm) by the same experiment.

Choline end group showed in **Table 2**, two set of signals probably due to conformational equilibrium: Multiplets assigned to ^{21}H (4.54 ppm), ^{22}H (3.33 ppm), and ^{23}H (2.74 ppm), correlated in COSY, and another set was multiplets $^{21'}H$ (4.76 ppm), $^{22'}H$ (3.85 ppm) and a singlet $^{23'}H$ (3.21 ppm).

The HSQC experiment allowed the direct allocation of carbon atoms linked to hydrogens, confirming the assignation of the proton signals overlapped in the ^{1}HNMR experiment. The correlation of carbon atom $^{11'}C$ (65.7 ppm) with H_a' (4.63 ppm) and H_b' (4.52 ppm); correlation between $^{11''}C$ (67.8 ppm) and H_a'' and H_b''; and correlation between carbon ^{21}C at (62.6 ppm) and ^{21}H at (4.54 ppm), are observed in **Table 2**.

PTOBDME-choline							**PTOBEE-choline**				
Observed chemical shifts			**Calc. chemical shifts**				**Observed chemical shifts**		**Calc. chemical shifts**		
Atom ^{1}H(ppm)			**Atom ^{13}C(ppm)**				**Atom ^{1}H(ppm)**		**Atom ^{13}C(ppm)**		
	DMSO		**DMSO**	**^{1}H calc**	**^{13}C calc**		**DMSO**		**DMSO**	**^{1}H calc**	**^{13}C calc**
^{21}H, $^{21'}H$	4.54, 4.76	^{21}C $^{21'}C$	62.6 58.8	4.69	58.1	^{13}H $^{13'}H$	*4.56* 4.75	^{13}C $^{13'}C$	58.8 58.5	4.69	58.1
^{22}H, $^{22'}H$	3.33 3.85	^{22}C $^{22'}C$	55.6 64.0	3.70	66.5	^{14}H $^{14'}H$	*3.32* 3.84	^{14}C $^{14'}C$	55.0	3.70	66.5
^{23}H, $^{23'}H$	2.74 3.21	^{23}C $^{23'}C$	43.2 53.0	3.30	54.4	^{15}H $^{15'}H$	2.74 3.22	^{15}C $^{15'}C$	42.5 52.7	3.30	54.4

Table 2. Observed ^{1}H and ^{13}C-NMR chemical shifts (ppm), in DMSO-d6, for the -N, N, N-trimethylethan- 1-ammonium (Choline) oxy benzoate hydrochloride end group, in Polyester PTOBDME-choline and Polyester PTOBEE-choline, and theoretical calculated values.

4.2. Structural characterization of PTOBEE-choline

The assignment of the ^{1}H and ^{13}C-NMR chemical shifts, in $CDCl_3$ and DMSO-d_6, of the monomeric unit and the end groups of PTOBEE-choline are given in **Table 3**, with the predicted values calculated by ChemDraw Professional [10]. Similar notations as those designated for precursor cholesteric liquid crystal PTOBEE [4] have been used.

In the ^{1}H-NMR experiment in CDCl3, observed chemical shifts are ^{12}H singlet at (8.34 ppm), ^{8}H doublet at (7.34 ppm), ^{7}H doublet at (8.16 ppm), $^{8'}H$ doublet at (7.36 ppm) and $^{7'}H$ doublet at (8.18 ppm). Multiplets at 5.46 and at 5.25ppm are interpreted as H_c' and $H_{c'}$ respectively. The double doublet at 4.60 ppm is assigned to H_a' and correlates in COSY with H_c' signal. An overlapped signal at 4.53 ppm is identified as H_b', with COSY and TOCSY cross signal

Set of signal of system (′) and (″)						Set of signal of system without apostrophe ( )						Calculated chemical shifts	
Atom	^{1}H(ppm)		Atom	^{13}C(ppm)		Atom	^{1}H(ppm)		Atom	^{13}C(ppm)		Atom	Atom
	$CDCl_3$	DMSO		$CDCl_3$	DMSO		$CDCl_3$	DMSO	DMSO	$CDCl_3$	DMSO	^{1}H	^{13}C
$^{12'}H$	8.34	8.35	$^{12'}C$	130.4	130.1	^{12}H	8.34	8.35	^{12}C	130.4	130.0	8.04	130.2
			$^{11'}C$	133.8	133.2				^{11}C	132.2	131.6		135.4
			$^{10'}C$	163.6	163.3				^{10}C	163.6	163.3		165.2
			$^{9'}C$	154.5	154.2				^{9}C	154.5	153.8		155.6
$^{8'}H$	7.36	7.48, 7.50	$^{8'}C$	121.7	121.7	^{8}H	7.34	7.53, 7.51	^{8}C	121.7	122.0	7.26	121.5
$^{7'}H$	8.18	8.08, 8.06	$^{7'}C$	131.5	130.6	^{7}H	8.16	8.11, 8.09	^{7}C	131.5	130.6	8.13, 8.11	130.3
			$^{6'}C$	128.3	128.7				^{6}C	127.9	127.3		126.9
			$^{5'}C$	165.4	166.4				^{5}C	165.4	164.7		165.9
H_c'	5.46	5.38	$^{4'}C$	73.8	73.1	H_c	5.25	5.20	^{4}C	75.1	74.4	4.55	72.5
H_c''	4.15	4.36	$^{4''}C$		61.6*							3.81	73.0
H_a', H_b'	4.60, 4.53	4.63, 4.52	$^{3'}C$	65.6	64.8	H_a, H_b	3.76, 3.74	3.94, 3.91	^{3}C	45.23	45.6	4.80, 4.55	67.2
H_a'', H_b''	4.53	4.52 *	$^{3''}C$	67.8	67.1							4.53, 4.28	70.5
H_d'	1.90	1.86	$^{2'}C$	24.4	23.0	H_d	1.86	1.81	^{2}C	24.4	24.2	1.75	23.5
H_d'', H_e''	1.88, 1.13	1.96, 1.80	$^{2''}C$		*							1.48	26.8
$^{1'}H$	1.09	1.02	$^{1'}C$	9.8	9.2	^{1}H	1.03	0.95	^{1}C	9.6	9.8	0.96	7.8
$^{1''}H$	1.13	1.04*	$^{1''}C$		8.73*							0.96	7.6

*Overlapped signal

Table 3. Observed and calculated ^{1}H and ^{13}C-NMR chemical shifts (ppm) for polyester PTOBEE-choline in DMSO-d_6 and $CDCl_3$. Repeating unit and the aliphatic end group.

with H_a'. At 4.15, a weak multiplet is assigned to H_c'', it presented COSY correlation with signal 4.53 ppm, indicating the presence of H_a'' and H_b''. The two double doublets at 3.76 and 3.74 ppm were identified as H_a and H_b and presented the expected COSY correlation with H_c (5.25 ppm). The overlapped signal at 1.90 ppm is identified as H_d', with cross signal with H_c'. A very weak COSY cross signal between 4.15 and H_d''(1.88 ppm) is observed. Triplet at 1.09 ppm is due to $^{1'}$H, with TOCSY correlation with H_c', while triplet at (1.03 ppm) is ^{1}H, with TOCSY correlation with H_c. The weak triplet at 1.13 ppm corresponded with $^{1''}$H. As in PTOBDME-choline, the choline end group shows, in **Table 2**, two set of signals due to conformational equilibrium. Multiplets ^{13}H, ^{14}H are observed at 4.56 and 3.32 ppm, respectively, and ^{15}H at 2.74 ppm, correlated in COSY experiments, and another set was $^{13'}$H and $^{14'}$H multiplets at 4.75 and 3.84 ppm, respectively, singlet $^{15'}$H at 3.22 ppm.

HSQC experiment was performed to determine the chemical shift of carbons bonded to the assigned hydrogen. The complex signal at 4.53 in proton presented several correlations with carbons. H_a'(4.60 ppm) and H_b' (4.53 ppm) showed correlation with carbon $^{3'}$C (65.6 ppm). Another correlation with overlapped signal at 4.53 ppm $H_a''H_b''$ was observed with carbon $^{3''}$C (67.8 ppm). Signals corresponding to ^{1}C, ^{2}C, and ^{4}C of aliphatic end group were not observed due to the low concentration. ^{13}C-NMR experiment allowed the assignation of the carbons not attached to hydrogens matching the calculated model.

4.3. Structural characterization of PTOBDME-ammonium

The structure of PTOBDME-ammonium, as depicted **II** in **Figure 3**, is confirmed by ^{1}H and ^{13}C-NMR, with the chemical shifts given in **Table 4**. In the aromatic zone of the ^{1}H-NMR spectrum of PTOBDME-ammonium, in DMSO-d_6, a singlet at 8.36 ppm belongs to ^{20}H and doublets at 7.50 and 8.07 ppm are assigned to $^{16'}$H and $^{15'}$H, respectively, and doublets at 7.57 and 8.13 ppm to ^{16}H and ^{15}H. In the spacer zone where methylene and methines attached to oxygen are observed, a multiplet at 5.45 ppm, and the double doublets at 4.64 ppm, 4.48 ppm correspond to H_c', H_a', and H_b', respectively; these signals present correlation signals of COSY and are related with other aliphatic signals: H_d', H_e' (1.81 ppm) and H_f', H_g' (1.42 ppm) by TOCSY. Multiplet at 5.26 ppm is assigned to H_c and double doublets at 3.94 and 3.88 ppm, to H_a and H_b, they show COSY correlations and are related with signals H_d H_e (1.77 ppm) and H_f H_g (1.33 ppm), in the TOCSY experiment. In the set of signals due to aliphatic end group, H_a'', H_b'', and H_c'' are overlapped with H_b' (4.48 ppm) and with ^{21}H (4.38 ppm), according to TOCSY correlations observed for signal H_b' (4.48 ppm) and not observed for H_a' (4.63 ppm) and confirmed by HSQC. Aliphatic signals at 1.81 ppm (H_d', H_e') and 1.42 ppm (H_f', H_g') have TOCSY correlation with 5.45 ppm (H_c'), also COSY correlation. Signals at 1.77 ppm (H_d H_e) and 1.33 ppm (H_f H_g) show TOCSY correlation with H_c (5.26 ppm). The signal at 1.33 ppm cannot be observed in the ^{1}H sprectrum due to the overlapping with CH_2, but it was clearly observed in TOCSY 2D. Signals at 1.91 and 1.78 ppm, related with H_c''(4.38 ppm) by COSY and TOCSY, are assigned to H_d'' and H_e'' and are also related with H_f''(1.51 ppm) and H_g''(1.42 ppm) by the same experiment.

Ammonium end group shows ^{23}H, ^{22}H, ^{24}H multiplets at 3.28 ppm, 2.17 ppm, and 2.79 ppm, respectively . ^{23} H at 3.28 ppm was overlapped with signal of H_2O of the deuterated solvent,

Set of signal of system (′) and (″)				Set of signal of system without apostrophe ( )				Calculated chemical shift	
Atom	**^{1}H (ppm**	**Atom**	**^{13}C(ppm)**	**Atom**	**^{1}H(ppm)**	**Atom**	**^{13}C(ppm)**	**^{1}H(ppm)**	**^{13}C(ppm)**
$^{20'}$H	8.36	$^{20'}$C	130.4	^{20}H	8.36	^{20}C	130.4	8.04	130.2
		$^{19'}$C	133.3			^{19}C	133.3		135.5
		$^{18'}$C	163.5			^{18}C	163.4		165.2
		$^{17'}$C	153.8			^{17}C	154.3		155.7
$^{16'}$H	7.50	$^{16'}$C	122.1	^{16}H	7.57	^{16}C	122.4	7.26	121.5
$^{15'}$H	8.07	$^{15'}$C	131.0	^{15}H	8.13	^{15}C	131.0	8.13;8.11	130.3
		$^{14'}$C	128.9			^{14}C	127.6		127.0
		$^{13'}$C	166.6			^{13}C	164.8		166.0
H_c'	5.45	$^{12'}$C	72.6	H_c	5.26	^{12}C	73.4	4.55	70.4
H_c''	4.38	$^{12''}$C	60.4					3.81	70.9
H_a', H_b'	4.64, 4.48	$^{11'}$C	66.0	H_a, H_b	3.94, 3.88	^{11}C	46.4	4.80, 4.55	67.6
H_a'', H_b''	4.48	$^{11''}$C	67.8					4.53, 4.28	70.9
H_d', H_e'	1.81	$^{10'}$C	30.3	H_d, H_e	1.77	^{10}C	31.3	1.71	30.8
H_d'', H_e''	1.91 1.78	$^{10'}$C	33.6					1.44	34.1
H_f', H_g'	1.42	$^{9'}$C	24.6	H_f, H_g	1.33	^{9}C	24.3	1.29	23.4
H_f'', H_g''	1.51;1.42	$^{9''}$C	25.3					1.29	23.2
$^{8'}$H	1.22	$^{8'}$C	28.6 m*	^{8}H	1.22	^{8}C	28.6 m*	1.29	29.7
$^{7'}$H	1.22	$^{7'}$C	28.6 m*	^{7}H	1.22	^{7}C	28.6 m*	1.29	29.7
$^{6'}$H	1.22	$^{6'}$C	28.6 m*	^{6}H	1.22	^{6}C	28.6 m*	1.26	29.7
$^{5'}$H	1.22	$^{5'}$C	28.5 m*	^{5}H	1.22	^{5}C	28.5 m*	1.26	29.7
$^{4'}$H	1.22	$^{4'}$C	28.1 m*	^{4}H	1.22	^{4}C	28.1 m*	1.26	29.4
$^{3'}$H	1.22	$^{3'}$C	31.3	^{3}H	1.22	^{3}C	31.3	1.26	31.9
$^{2'}$H	1.22	$^{2'}$C	22.1	^{2}H	1.22	^{2}C	22.1	1.26	22.8
$^{1''}$H	0.84	$^{1'}$C	14.0	^{1}H	0.84	^{1}C	14.0	0.86	14.1

The symbol (′) and with no apostrophe ( ) distinguish the two independent systems of the repeating unit, the symbol (″) is used to mark the signals of the aliphatic end group.*Signal of ^{13}C at 28.8 ppm is a multiplet from 28.9 to 28.7.

Table 4. ^{1}H and ^{13}C-NMR chemical shifts (ppm) observed and calculated for the repeating unit of polyester PTOBDME-ammonium chloride and the aliphatic end group.

and it was assigned due to the COSY and TOCSY correlations with signals at 4.38 ppm (^{21}H) and at 2.17 ppm (^{22}H) and HSQC correlation with ^{23}C at 54.0 ppm. ^{21}H signal was overlapped at 4.38 ppm, and it was identified by COSY correlations with 2.17 ppm (^{22}H) and TOCSY

correlations with 3.28 ppm (^{21}H). The polymer holds positive charge due to ammonium proton ^{25}H observed at 10.33 ppm.

The HSQC experiment confirmed the direct assignation of carbon atom $^{11'}$C (66.0 ppm) linked to protons H_a' (4.63 ppm) and H_b' (4.48 ppm). Signal H_b' exhibits correlation with $^{11''}$C (67.8 ppm), linked to H_a'' and H_b''. Two cross signal are observed for H_c'' (4.38 ppm), one with carbon atom at $^{12''}$C (60.4 ppm) and another with ^{21}H linked to carbon atom ^{21}C (62.3 ppm). The correlations of carbon atom $^{10''}$C (33.6 ppm) with H_d''(1.91 ppm) and H_e''(1.78 ppm), and carbon atom $^{9''}$C (25.6 ppm) with H_f''(1.51 ppm) and H_g''(1.42 ppm) confirmed the previous assignation.

4.4. Structural characterization of PTOBEE-ammonium

Table 6 shows the assignation of ^{1}H and ^{13}C-NMR chemical shifts (ppm) observed of polyester PTOBEE-ammonium chloride and calculated for the repeating unit and the aliphatic end group. In the ^{1}H-NMR experiment, in CDC_{l3}, peaks observed at 8.34, 7.36, 7.34, 8.18, and 8.16 ppm are assigned to ^{12}H singlet, $^{8'}$H doublet, ^{8}H doublet and $^{7'}$H doublet, and ^{7}H doublet, respectively. Peak at 5.46 ppm is H_c' and 5.25 ppm is H_c. The double doublet at 4.60 ppm is interpreted as H_a' because of its shape and the COSY correlation with H_c'. An overlapped signal at 4.53 ppm is attributed to H_b', by COSY and TOCSY cross signal with H_a'. A weak multiplet at 4.15 ppm is assigned to H_c'', and this signal presented COSY correlation with H_b', indicating the presence of H_a'' and H_b''. The two double doublets at 3.76 and 3.74 ppm are identified as H_a and H_b and presented the expected COSY correlation with H_c. The overlapped signal at 1.90 ppm is H_d' correlated with H_c'. A very weak COSY cross signal is observed between H_c'' and 1.88 ppm (H_d''). Triplet signal at 1.09 ppm with TOCSY correlation with H_c' is interpreted as H_e', while triplet at 1.03 ppm with TOCSY correlation with H_c was assigned to H_e. The weak triplet at 1.13 ppm corresponds to H_e''.

Signals of proton ammonium end group in DMSO-d_6 are observed at (**Table 5**): ^{16}H singlet (2.81 ppm), ^{15}H multiplet (3.25 ppm), ^{14}H multiplet (2.18 ppm), and ^{13}H multiplet overlapped at (4.39 ppm) but presented COSY correlations with 2.18 ppm and TOCSY correlations with 3.25 ppm. The compound is positively charged, with the ammonium proton ^{17}H observed at 10.3 ppm in DMSO-d_6 and 13.2 ppm in $CDCl_3$.

HSQC experiment exhibits several correlations of the complex proton signal at 4.53 ppm, carbon atoms. Double doublet H_a'(4.60 ppm) H_b' (4.53) correlates with $^{3'}$C at (65.6 ppm). Another correlation is observed between proton H_a'' and $^{3''}$C (67.8 ppm). Correlation between the overlapped signal of proton ^{13}H (4.39 ppm), within the ammonium end group, and ^{13}C (61.9 ppm) in $CDCl_3$ is observed.

4.5. Structural characterization of PTOBUME-amide

The structures of undec-10-enamide, 10-11-epoxy-undecanamide, and 10,11-dihydroxyundecanamide (**III**, **IV** and **V** in **Figure 4**) were confirmed by ^{1}H-NMR, ^{13}C-NMR, registered in DMSO-d_6 at 25°C in a Bruker 300 MHz NMR spectrometer. Chemical shifts and Mass spectrometry results are given in Section 2.3.

The structure of PTOBUME-amide, **VII** in **Figure 4**, has also been confirmed by ^{1}H-NMR, ^{13}C-NMR, COSY and HSQC, obtained in VARIAN 400 and 500 MHz spectrometers, also at room

PTOBDME-Ammonium						PTOBEE-Ammonium							
Observed chemical shifts				Calc. chemical shifts		Observed chemical shifts						Calc. chemical shifts	
Atom	^{1}H (ppm)	Atom	^{13}C (ppm)	^{1}H (ppm)	^{13}C (ppm)	Atom	^{13}C (ppm)	^{1}H (ppm)	Atom	^{1}H (ppm)	^{13}C (ppm)	^{1}H (ppm)	^{13}C (ppm)
	DMSO		DMSO				DMSO	$CDCl_3$		DMSO	$CDCl_3$		
^{21}H	4.38	^{21}C	62.3	4.25	63.0	^{13}H	4.39	4.49	^{13}C	61.3	61.9	4.25	63.0
^{22}H	2.17	^{22}C	23.8	2.19	22.5	^{14}H	2.18	2.42	^{14}C	23.1	24.5	2.19	22.5
^{23}H	3.28	^{23}C	54.0	3.24	55.2	^{15}H	3.25	3.14	^{15}C	53.8	55.5	3.24	55.2
^{24}H	2.79	^{24}C	42.5	2.90	45.0	^{16}H	2.81	2.82	^{16}C	41.9	43.1	2.90	45.0
^{25}H	10.33			7.0		^{17}H	10.33	13.2				7.0	

Table 5. ^{1}H and ^{13}C-NMR chemical shifts (ppm) observed for the 3-dimethylamine-1-propyl benzoate hydrochloride end group in polyester PTOBDME-ammonium and polyester PTOBEE-ammonium, and calculated values.

Set of signal of system (′) and (″)						Set of signal of system without apostrophe ( )						Calculated chemical shift	
Atom	^{1}H(ppm)		Atom	^{13}C(ppm)		Atom	^{1}H(ppm)		Atom	^{13}C(ppm)		Atom	Atom
	$CDCl_3$	DMSO		$CDCl_3$	DMSO		$CDCl_3$		DMSO	$CDCl_3$	DMSO	^{1}H	^{13}C
$^{12'}$H	8.34	8.36	$^{12'}$C	130.4	129.9	^{12}H	8.34	8.36	^{12}C	130.4	129.9	8.04	130.2
			$^{11'}$C	133.8					^{11}C	132.2			135.4
			$^{10'}$C	163.6					^{10}C	163.6			165.2
			$^{9'}$C	154.5					^{9}C	154.5			155.6
$^{8'}$H	7.36	7.53	$^{8'}$C	121.7	121.7	^{8}H	7.34	7.53	^{8}C	121.9	121.7	7.26	121.5
$^{7'}$H	8.18	8.13	$^{7'}$C	131.5	130.4	^{7}H	8.16	8.11	^{7}C	131.5	130.4	8.13, 8.11	130.3
			$^{6'}$C	128.3					^{6}C	127.9			126.9
			$^{5'}$C	165.4					^{5}C	165.4			165.9
H_c'	5.46	5.39	$^{4'}$C	73.8	73.02	H_c	5.25	5.20	^{4}C	75.1	74.4	4.55	72.5
H_c''	4.15	4.40	$^{4''}$C		*							3.81	73.0
H_a', H_b'	4.60, 4.53	4.64 4.53	$^{3'}$C	65.6	64.6	H_a, H_b	3.76, 3.74	3.96, 3.92	^{3}C	45.23	45.6	4.80, 4.55	67.2
H_a'', H_b''	4.53	4.48*	$^{3''}$C	67.8	*							4.53, 4.28	70.5
H_d'	1.90	1.86	$^{2'}$C	24.4	23.06	H_d	1.90	1.82	^{2}C	24.4	24.1	1.75	23.5
H_d'', H_e''	1.88, 1.13	1.90, 1.86*	$^{2''}$C		*							1.48	26.8
$^{1'}$H	1.09	1.04	$^{1'}$C	9.8	8.73	H_e	1.03	0.96	^{1}C	9.6	8.38	0.96	7.8
$^{1''}$H	1.13	1.06*	$^{1''}$C		8.73*							0.96	7.6

*Overlapped signal.

Table 6. ^{1}H and ^{13}C-NMR chemical shifts (ppm) observed for polyester PTOBEE-ammonium chloride, both the repeating unit and the aliphatic end group, in DMSO-d6 and in $CDCl_3$, and calculated values.

temperature. The solvent used were DMSO-d_6 and $CDCl_3$ from Merck KGaA (Darmstadt, Germany). The spectra were processed and analyzed with the help of MestReNova 11.0.4 [9]. The chemical shifts are given in **Table 7**. Theoretical values predicted by ChemDraw Professional, v. 15.1.0.144. Tilted values are chemical shifts registered in $CDCl_3$.

4.6. Structural characterization of PTOBEE-amide

The structure of PTOBEE-amide, **VI** in **Figure 5**, has also been confirmed by ^{1}H-NMR, ^{13}C-NMR, COSY and HSQC, obtained in VARIAN 400 and 500 MHz spectrometers, at room temperature. The solvent used was DMSO-d_6 from Merck KGaA (Darmstadt, Germany). The experimental chemical shifts analyzed from the spectra are given in **Table 8**. Theoretical values predicted by ChemDraw Professional, v. 15.1.0.144.

System (′)				**System without apostrophe ( )**				**Theoretical chemical shifts**			
Atom	**^{1}H**	**Atom**	**^{13}C**	**Atom**	**^{1}H**	**Atom**	**^{13}C**	**Atom**	**^{1}H**	**Atom**	**^{13}C**
$^{19'}$H	8.36	$^{19'}$C		^{19}H	8.36	^{19}C	*130.4*	^{19}H	8.04	^{19}C	130.2
		$^{18'}$C				^{18}C	*133.7*			^{18}C	135.5
		$^{17'}$C				^{17}C	*163.7*			^{17}C	165.2
		$^{16'}$C				^{16}C	*154.7*			^{16}C	153.7
$^{15'}$H	8.07	$^{15'}$C		^{15}H	8.07	^{15}C	*121.6*	^{15}H	7.52	^{15}C	121.5
$^{14'}$H	7.50	$^{14'}$C		^{14}H	7.50	^{14}C	*131.3*	^{14}H	8.18	^{14}C	130.3
		$^{13'}$C				^{13}C	*128.2*			^{13}C	126.9
		$^{12'}$C				^{12}C	*165.7*			^{12}C	165.9
H_c'	5.76	$^{11'}$C		H_c	5.45	^{11}C		H_c	5.16	^{11}C	70.3
H_a', H_b'	4.95, 4.30	$^{10'}$C		H_a, H_b	4.23, 4.18	^{10}C		H_a,H_b	4.78, 4.53	^{10}C	66.0
H_d', H_e'	1.74	$^{9'}$C		H_d, H_e	1.55	^{9}C		H_d, H_e	1.67	^{9}C	30.7
H_f', H_g'	1.37	$^{8'}$C		H_f, H_g	1.22	^{8}C		H_f, H_g	1.25	^{8}C	23.3
$^{7'}$H	1.22	$^{7'}$C		^{7}H	1.22	^{7}C		^{7}H	1.25	^{7}C	29.6
$^{6'}$H	1.22	$^{6'}$C		^{6}H	1.22	^{6}C		^{6}H	1.26	^{6}C	29.6
$^{5'}$H	1.22	$^{5'}$C		^{5}H	1.22	^{5}C		^{5}H	1.30	^{5}C	28.9
$^{4'}$H	1.22	$^{4'}$C		^{4}H	1.22	^{4}C		^{4}H	1.30	^{4}C	28.6
$^{3'}$H	1.52	$^{3'}$C		^{3}H	1.52	^{3}C		^{3}H	1.53	^{3}C	25.3
$^{2'}$H	2.28	$^{2'}$C		^{2}H	2.28	^{2}C		^{2}H	2.34	^{2}C	38.7
NH_2'	7.0	$^{1'}$C		NH_2	7.0	^{1}C		NH_2	7.03	^{1}C	173.6
Experimental signals “end group”								Theoretical chemical shifts end group			
H_c''	4.18			$^{11''}$C				H_c''	4.57	$^{11''}$C	73.6

System (′)				System without apostrophe ( )				Theoretical chemical shifts			
Atom	**^{1}H**	**Atom**	**^{13}C**	**Atom**	**^{1}H**	**Atom**	**^{13}C**	**Atom**	**^{1}H**	**Atom**	**^{13}C**
H_a'', H_b''				$^{10''}C$				H_a'', H_b''	3.86, 3.80	$^{10''}C$	64.3
H_d'', H_e''	1.62			$^{9''}C$				H_d'', H_e''	1.67	$^{9''}C$	30.5
H_f'', H_g''	1.22			$^{8''}C$				H_f'', H_g''	1.25	$^{8''}C$	25.6
$^{7''}H$	1.22			$^{7''}C$				$^{7''}H$	1.25	$^{7''}C$	29.6
$^{6''}H$	1.22			$^{6''}C$				$^{6''}H$	1.26	$^{6''}C$	29.6
$^{5''}H$	1.22			$^{5''}C$				$^{5''}H$	1.30	$^{5''}C$	28.9
$^{4''}H$	1.22			$^{4''}C$				$^{4''}H$	1.30	$^{4''}C$	28.6
$^{3''}H$	1.52			$^{3''}C$				$^{3''}H$	1.53	$^{3''}C$	25.3
$^{2''}H$	2.28			$^{2''}C$				$^{2''}H$	2.34	$^{2''}C$	38.7
NH_2 "	10.7			$^{1''}C$				NH_2 "	7.03	$^{1''}C$	173.6
$\mathbf{CH}_2$	4.36			$\mathbf{C}H_2$		*61.2*		$\mathbf{CH}_2$	4.29	$\mathbf{C}H_2$	60.9
$\mathbf{CH}_3$	1.35			$\mathbf{C}H_3$		*14.3*		$\mathbf{CH}_3$	1.30	$\mathbf{C}H_3$	14.1

Table 7. ^{1}H and ^{13}C-NMR chemical shifts (ppm) observed and calculated for chiral Polyesteramide PTOBUME-amide.

System (′)				System without apostrophe ( )				Theoretical chemical shifts			
Atom	**^{1}H**	**Atom**	**^{13}C**	**Atom**	**^{1}H**	**Atom**	**^{13}C**	**Atom**	**^{1}H**	**Atom**	**^{13}C**
$^{12'}H$	8.32	$^{12'}C$	131.36	^{12}H	8.32	^{12}C	131.36	^{12}H	8.04	^{12}C	130.2
		$^{11'}C$				^{11}C				^{11}C	135.4
		$^{10'}C$				^{10}C				^{10}C	165.2
		$^{9'}C$				^{9}C				^{9}C	155.7
$^{8'}H$	8.08	$^{8'}C$	132.35	^{8}H	8.08	^{8}C	132.35	^{8}H	8.18	^{8}C	121.5
$^{7'}H$	7.45	$^{7'}C$	123.06	^{7}H	7.45	^{7}C	123.06	^{7}H	7.52	^{7}C	130.3
		$^{6'}C$				^{6}C				^{6}C	126.9
		$^{5'}C$				^{5}C				^{5}C	165.9
H_c'	5.67	$^{4'}C$		H_c	5.43	^{4}C		H_c	4.56	^{4}C	70.2
H_a', H_b'	4.63, 4.49	$^{3'}C$		H_a,H_b	4.32, 4.22	^{3}C		H_a,H_b	4.78, 4.53	^{3}C	66.5
H_d', H_e'	3.22, 3.10	$^{2'}C$		H_d, H_e	1.05	^{2}C		H_d, H_e	2.46	^{2}C	38.9
NH_2'	7.61	$^{1'}C$	17.47	NH_2	7.61	^{1}C		NH_2	7.03	^{1}C	173.6

Table 8. ^{1}H and ^{13}C-NMR chemical shifts (ppm) observed and calculated for chiral Polyesteramide PTOBEE-amide.

5. Thermal stability and differential scanning calorimetry (DSC)

The presence of choline group at the end of polymer chains causes in PTOBDME-choline a decrease in the thermal stability range compared to precursor PTOBDME. A 5% weight loss is observed for PTOBDME-choline at 230°C, while PTOBDME loses 5% weight at about 280°C. The thermal stability of PTOBEE-Choline is similar to that of polyester PTOBEE. PTOBEE-choline has 5% weight loss at 281°C, and PTOBEE at 280°C (see **Figures 6** and **7**). In the thermal stability curve of PTOBDME-choline, the first degradation step observed at 230°C is followed by two other weight loss step at 280 and 448°C. Two decomposition steps are observed at 280 and 466°C in PTOBEE-choline.

In the DSC experiment of PTOBDME-choline, performed at 10°C/min, **Figure 6(b)**, a glass transition can be observed at 58.2°C, in the first heating run, and a weak endothermic peak at 99.5°C is interpreted as due to the first order transition from crystal phase to liquid crystal state. An exothermic peak at 171.2°C is also observed which is not explained, but the beginning of a second endothermic peak at 200°C can be attributed to fusion to the isotropic. In the cooling process, two exothermic peaks at 155°C and at 175 are observed, probably associated to crystal formation. In the second heating, a very broad endothermic peak at 100.2°C is observed again associated to the transition to liquid crystal mesophase.

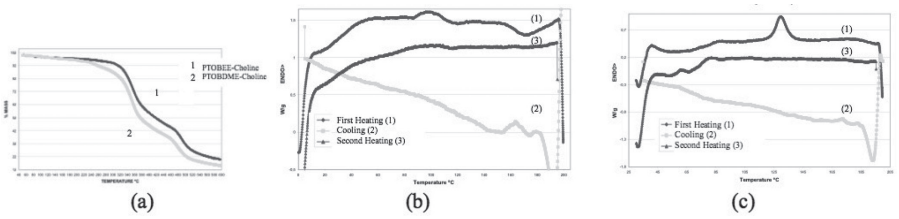

Figure 6. (a) Thermogravimetry of PTOBDME-choline and PTOBEE-choline; (b) DSC analysis of PTOBDME-choline and (c) DSC of PTOBEE-choline, both at 10°C/min.

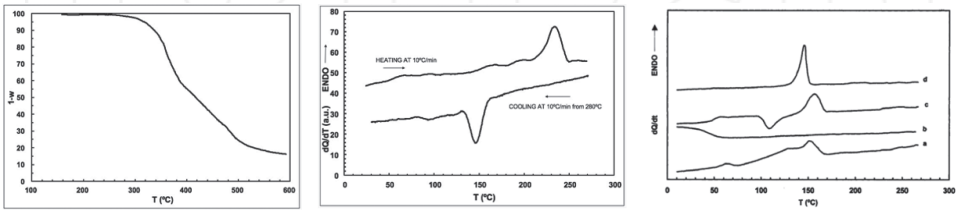

Figure 7. (I) Thermogravimetry of precursor PTOBDME; (II) DSC analysis of PTOBDME; (III) DSC of PTOBEE: (a) first heating process of the original sample, (b) subsequent cooling down, (c) second heating process; and (d) DSC of (—) PTOBEE. First heating run of the original sample. All at 10°C/min.

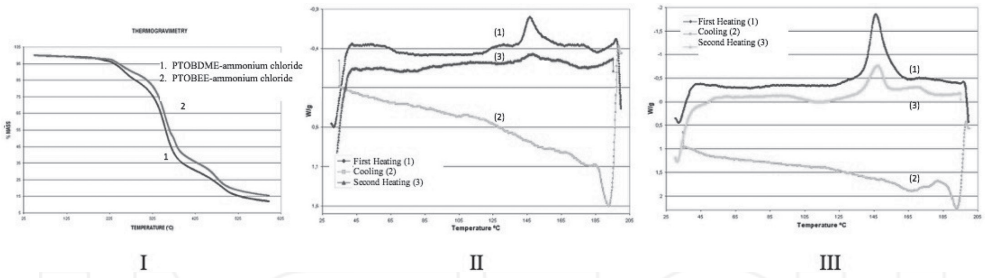

Figure 8. (I) Thermogravimetric curve of PTOBDME-ammonium and PTOBEE-ammonium; (II) DSC analysis of PTOBDME-ammonium; (III) and PTOBEE-ammonium chloride. All at 10°C/min of.

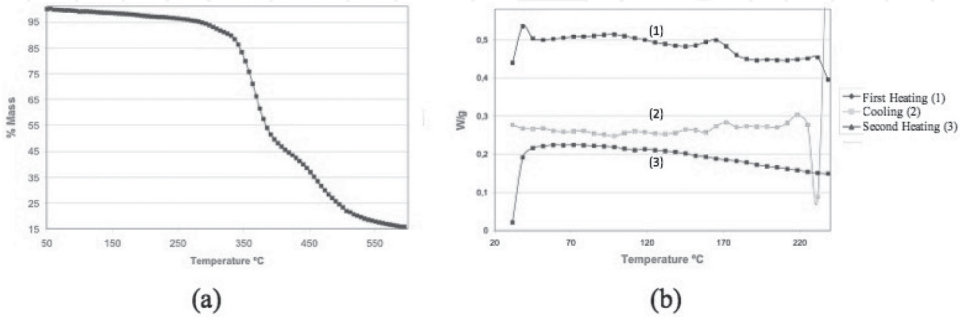

Figure 9. (a) Thermogravimetric curve of PTOBUME-amide; (b) DSC analysis of PTOBUME-amide.

In the DSC experiment of PTOBEE-choline at (10°C/min), **Figure 6(c)**, a glass transition can be observed at 60°C, and an endothermic peak at 130.2°C is attributed to the transition crystal to liquid crystal. A decreasing of baseline from 183.7°C to the end of heating was also observed in the first heating run due to a nonconcluded endothermic process or to the beginning of degradation to the polymer. A broad exothermic peak observed the cooling around 145°C would correspond to a crystallization from the mesophase state. In the second heating, only two glass transitions can be observed at 65 and 85°C.

The presence of ammonium chloride group at the end in the polymer chains, in **Figure 8-I**, produces a decrease of the thermal stability range compared to precursor polyesters. At 278°C, PTOBEE-ammonium chloride loses 10% weight and PTOBDME-ammonium chloride at 260° C, while precursor PTOBDME and PTOBEE at 310°C. In the thermal stability curve of the ammonium-polymers, the first degradation step observed at 228 and 230°C, respectively, was not observed in PTOBEE and PTOBDME. The two next inflexion points at 310 and 311°C and 466 and 471°C were equivalents to the observed in the precursor polyesters, which would indicate the same type of decomposition to principal core of the chain.

In the DSC experiment of PTOBDME-ammonium chloride, at 10°C/min, **Figure 8-II**, a very broad exothermic peak centered at 96.8°C, is observed in the first heating, associated to low enthalpy value, which can be attributed to crystal to crystal transitions, involving molecular reordering between crystalline phases. An endothermic peak at 146.9°C is interpreted due to the transition to liquid crystal mesophase; finally, an exothermic peak at 186.8°C is observed. In the cooling run, very weak exothermic peaks at 154.4 and at 104.1°C were observed due crystallization process. In the second heating, a broad exothermic peak centered at 75.2°C, an endothermic peak at 149.1°C, and finally, an exothermic peak at 179.8°C were observed again.

The DSC experiment of PTOBEE ammonium choride, at 10°C/min, **Figure 8-III**, shows in the first heating run a broad exothermic peak centered at 69.1°C, and a very strong endothermic peak at 146.2°C due to the fusion transition from crystalline phase to liquid crystal mesophase, and finally, a weak endothermic peak at 173.3°C, perhaps due to a partial fusion to isotropic. During the cooling, an exothermic peak appeared at 166°C would correspond to a crystallization from the mesophase state, and in the second heating, the broad exothermic peak observed in the first heating was observed to higher temperature centered at 114.8°C; the two endothermic peaks were again observed at 147.6 and 170.1°C.

The thermogravimetric curve and the DSC analysis of PTOBUME-amide are given in **Figure 9**. At 265°C, it loses 5% weight. At 340°C, a first decomposition step begins, followed by another three at 400, 450, and 510°C. In the first heating of the DSC, an endothermic peak is observed at 160°C interpreted as the transition to the mesophase state. In the cooling run, several week exothermic peaks could be associated to crystal formation processes.

6. Optical characterization

6.1. Optical activity of PTOBDME-ammonium and PTOBEE-ammonium

As in the polyester precursors PTOBEE-ammonium chloride and PTOBDME-ammonium chloride presented an unexpected optical activity and chiral morphology, although they were synthesized starting from equimolar quantities of TOBC and the racemic mixture of the corresponding glycol. The obtained chirality has been evaluated by optical rotatory dispersion, in **Figure 10**, the values of optical activity are given as $[\alpha]^{25°C}$, at different wavelengths. **Table 9** shows the measured values.

In the optical characterization of precursor cholesteric liquid crystal polyesters [1, 3], even an increase of chirality was observed for a second fraction of the polymer, obtained by precipitation, after days of reaction of the liquors mother with respect to the initial first fraction of the polymer. The optical activity of PTOBDME-choline, PTOBEE-choline, PTOBUME-amide and PTOBEE-amide, has not been studied at the end of the present article but will be reported in the future.

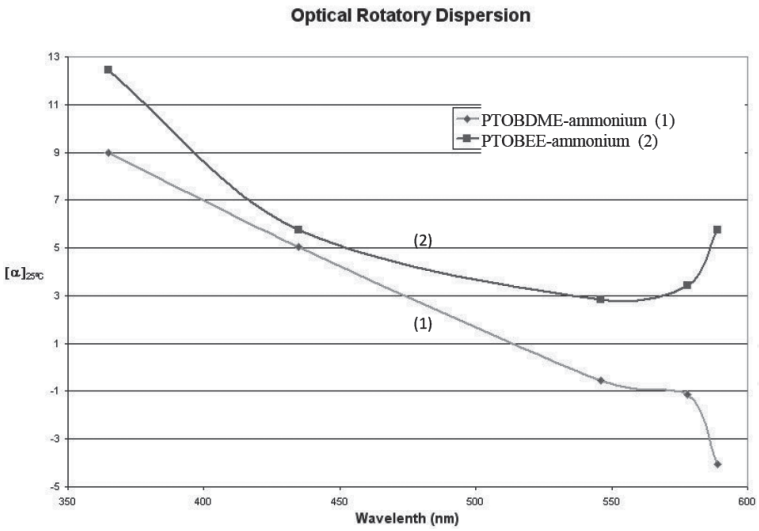

Figure 10. Optical activity of PTOBDME-ammonium chloride and PTOBEE-ammonium choride. Expressed as $[\alpha]^{25°C}$ in DMSO-d_6 at different wavelengths.

Polymers (0.2 g/100 ml in DMSO)	Hg (365 nm)	Hg (435 nm)	Hg (546 nm)	Hg (578 nm)	Na (589 nm)
PTOBEE-ammonium chloride	+12.44°	+5.75°	+2.85°	+3.44°	+5.75°
PTOBDME-ammonium chloride	+9.00	+5.06	−0.55	−1.15	−4.04

Table 9. Optical activity of PTOBDME-ammonium and PTOBEE-ammonium, expressed by optical rotatory dispersion.

7. Conclusions

The synthetic methods of six new multifunctional cationic cholesteric liquid crystal polymers designed as PTOBDME-choline $[(C_{34}H_{36}O_8)_n{-}C_5H_{13}N]$; PTOBEE-choline $[(C_{26}H_{20}O_8)_n{-}C_5H_{13}N]$; PTOBDME-ammonium $[(C_{34}H_{36}O_8)_n{-}C_5H_{13}N]$; PTOBEE-ammonium $[(C_{26}H_{20}O_8)_n{-}C_5H_{13}N]$; PTOBUME-amide $(C_{33}H_{33}O_9N)_n$ and PTOBEE-amide $(C_{26}H_{19}O_9N)_n$ are given and their characterization by ^1H, ^{13}C-NMR, COSY, and HSQC is reported.

The NMR analysis let us to conclude that the enantiomeric polymer chains present stereo regular head-tail, isotactic structure, explained in terms of the higher reactivity of the primary hydroxyl group in the glycol, with respect to the secondary one, through the polycondensation reaction.

According to our previous experience, each enantiomer, with two independent sets of signals observed by ^1H and ^{13}C-NMR, differentiated with apostrophe (′) and without it ( ), could be attributed to two diastereomeric conformers: *gg* and *gt*, related with two possible staggered conformations, of the torsion along the chemical bond containing the asymmetric carbon atom

in the spacer, along the copolymer backbone, with two possible helical screw sense of the polymer chain and in all the studied polymers. Chirality in racemic PTOBDME was proposed to be due to the kinetic resolution of a preferable helical diastereomer, such as S*gt*, with respect to the possible four forms, while the R/S ratio of asymmetric carbon atoms remained 50:50.

The presence of choline group or ammonium chloride groups at the end of polymer chains causes in precursor polyesters a decrease in their thermal stability range. PTOBDME-choline losses 5% weight at 230°C (PTOBDME at 280°C). The thermal stability of PTOBEE-choline is similar to that precursor PTOBEE, with 5% weight loss at 281°C.

At 260°C, PTOBDME-ammonium loses 10% weight and PTOBEE-ammonium at 278°C (precursor PTOBDME and PTOBEE at 310°C).

All the synthetized cationic liquid crystal polymers show in DSC an endothermic peak assigned to the first order transition from crystalline phase to liquid crystal mesophase: PTOBDME-choline at 99.5°C; PTOBEE-choline at 130.2°C; PTOBDME-ammonium at 146.9°C; and PTOBEE-ammonium at 146.2°C.

At 265°C, PTOBUME-amide loses 5% weight. At 340°C, it has a first decomposition step, followed by another three at 400, 450, and 510°C. In the DSC first heating, it shows the endothermic peak due to the mesophase transition at 160°C.

Optical ORD values are provided for the second fractions of PTOBDME-ammonium and PTOBEE-ammonium.

Acknowledgements

The author thanks Dr. Javier Sanguino Otero for his valuable help during the development of this Project. She also thanks the financial support obtained in the Project "Nuevos vectores no virales basados en polímero cristal-líquido colestérico (PCLC) y su uso para transfección génica". PTR1995-0760-OP.

Author details

Mercedes Pérez Méndez

Address all correspondence to: perezmendez@ictp.csic.es

Instituto de Ciencia y Tecnología de Polímeros (ICTP), CSIC, Madrid, Spain

References

[1] Pérez Méndez M, Sanguino Otero J. Cholesteric Liquid-Crystal Copolyester, Poly[oxy-carbonyl-1,4-phenylene-oxy-1,4 terephthaloyl-oxy-1,4-phenylene-carbonyloxy

(1,2-dodecane)] $[C_{34}H_{36}O_8]_n$, Synthesized from Racemic Materials: Kinetics, Structure and Optical Characterization. International Journal of Engineering Research and Applications (IJERA). July 2015;**5**(7, Part-2):48-62. ISSN: 2248-9622, http://www.ijera.com/papers/Vol5_issue7/Part%20-%202/H57024862.pdf

[2] Fayos J, Sanchez-Cortes S, Marco C, Pérez-Méndez M. Journal of Macromolecular Science Part B Physics.Conformational analysis and molecular modeling of cholesteric liquid-crystal polyesters based on XRD, Raman and transition thermal analysis. Journal of Macromolecular Science Part B Physics. 2001;**40**:553-576

[3] Perez-Mendez M, Marsal R, Garrido L, Martin-Pastor M. Self-Association and Stereoselectivity in a Chiral Liquid-Crystal Colesteric Polymer Formed under Achiral Conditions. Macromolecules. 2003;**36**:8049-8055

[4] (a) Pérez-Méndez M, Marco C. New synthesis, thermal properties and texture of cholesteric poly[ethyl ethylene 4,4'-(terephthaloyldioxy)dibenzoate]. Acta Polymerica. 1997;**48**:502-506. (b) Pérez-Méndez M, Marco Rocha C. Process for obtaining cholesteric liquid crystals by stereoselective recrystallization. Patents: EP1004650-A, WO9831771-A, WO9831771-A1, AU9854863-A, ES2125818-A1, US6165382-A, MX9906732-A1, JP2001513827-W, AU739076-B, DE69824182-E

[5] (a) Bilibin AY, Ten'kovtsev AV, Piraner ON, Skorokhodov SS. Synthesis of highmolecular weight liquid crystal polyesters based on a polycondensation mesogenic monomer. Polymer Science U.S.S.R. 1984;**26**(12):2882-2890. (b) Bilibin AY, Skorokhodov SS. Rational path of the synthesis of liquid-crystalline highmolecular weight polyesters and their properties in solution. Macromolecular Symposia. 1989;**29**:9-23

[6] Pérez Méndez M, Rodríguez Martínez D, Fayos Alcañíz J. Structure of non-viral vectors based on cholesteric liquid-crystal polymers by SAXS. International Journal of Advancement in Engineering Technology, Management and Applied Science (IJAETMAS). 2016;**03**(11):27-41. ISSN 2349-3224, http://www.ijaetmas.com/wp-content/uploads/2016/11/IJ16M1031.pdf

[7] Pérez Méndez M, Hammouda B. SAXS and SANS investigation of synthetic cholesteric liquid-crystal polymers for biomedical applications. Journal of Materials Science and Engineering B. 2013;**3**(2):104-115

[8] Pérez Méndez M, Rodriguez Martinez D, King SM. pH-induced size changes in solutions of cholesteric liquid crystal polymers studied by SANS. Journal of Physics: Conference Series. Dynamics of Molecules and Materials-II. 2014;**554**(012011):1-11. IOP Publishing

[9] (a) Cobas JC, Sardina FJ, Concepts in Magenetic Resonance. Nuclear magnetic resonance data processing. MestRe-C: A software package for desktop computers. Concepts in Magenetic Resonance. 2003;**19**:80-96; (b) MestReNova 11.0.4, Mestrelab Research SL, Santiago de Compostela, Spain, www.mestrelab.com, 2017

[10] ChemDraw Professional, Version 15.1.0.144 (PerkinElmer Informatics 1985-2016)

[11] Knapp S, Levorse AT. Synthesis and Reactions of Iodo Lactams. Journal of Organic Chemistry; **53**:4006-4014

[12] Rani S, Vankar YD. An efficient one step dihydroxylation of 1,2-glycals with oxone in acetone. Tetrahedron Letters. 2003;**44**:907-909

[13] Corey PF, Ward FE. Buffered potassium peroxymonosulfate-acetone epoxidation of .Alpha.,.Beta.-unsaturated acids. The Journal of Organic Chemistry. 1986;**51**(10):1925-1926

[14] Zhu W, Ford WT. Oxidation of alkenes with aqueous potassium peroxymonosulfate and no organic solvent. The Journal of Organic Chemistry. 1991;**56**(25):7022-7026

[15] Ella-Menye JR, Sharma V, Wang G. New synthesis of chiral 1,3-oxazinan-2-ones from carbohydrate derivatives. The Journal of Organic Chemistry. 2005;**70**(2):463-469

INTECH